
GROUP-ON: BOOSTING ONE-SHOT SEGMENTATION WITH SUPPORTIVE QUERY

Hanjing Zhou^{1*}, Mingze Yin^{1*}, Jintai Chen^{2†}, Danny Chen³, Jian Wu^{1†}

¹Zhejiang University

²University of Illinois at Urbana-Champaign

³University of Notre Dame

{zhj85393, mzyin256, jtchen721}@gmail.com,
dchen@nd.edu, wujian2000@zju.edu.cn

ABSTRACT

One-shot semantic segmentation aims to segment query images given only ONE annotated support image of the same class. This task is challenging because target objects in the support and query images can be largely different in appearance and pose (*i.e.*, intra-class variation). Prior works suggested that incorporating more annotated support images in few-shot settings boosts performances but increases costs due to additional manual labeling. In this paper, we propose a novel approach for ONE-shot semantic segmentation, called GROUP-ON, which packs multiple query images in batches for the benefit of mutual knowledge support within the same category. Specifically, after coarse segmentation masks of the batch of queries are predicted, query-mask pairs act as pseudo support data to enhance mask predictions mutually, under the guidance of a simple Group-On Voting module. Comprehensive experiments on three standard benchmarks show that, in the ONE-shot setting, our GROUP-ON approach significantly outperforms previous works by considerable margins. For example, on the COCO-20ⁱ dataset, we increase mIoU scores by 8.21% and 7.46% on ASNet and HSNet baselines, respectively. With only one support image, GROUP-ON can be even competitive with the counterparts using 5 annotated support images.

1 Introduction

Recently, few-shot learning (FSL) has garnered significant attention due to its remarkable success in reducing the dependence on data annotations during the development of deep learning (DL) models. This paradigm offers an efficient way to deploy a DL model that can generalize well to new and unseen data by using only a sparing amount of category-identical reference data with manual labels. This is especially advantageous for tasks that require costly manual annotations, such as pixel-wise segmentation of images. In a few-shot segmentation (FSS) practice, users require the segmentation model to segment unseen images (*i.e.*, query) with guidance from one or several references (*i.e.*, support) of the same class. Apparently, “one-shot setting” is the most annotation-effective solution, requiring the resource-intensive pixel-wise labeling of just one image. However, constrained by the limited information derived from just one manual annotation and the intrinsic diversity of the objects to be segmented, its performance often falls behind in other few-shot scenarios [1].

In this paper, we rethink one-shot segmentation scenarios and find that its performance can reach levels comparable to counterparts under the few-shot segmentation setting. Fig. 1(a) shows traditional one-shot segmentation scenarios. A great deal of users submit image queries into the segmentation model. For each category, the model retrieves one support image identical to the queried category, accompanied by annotations from human annotators for segmentation. To boost performance, few-shot segmentation setting is introduced as in Fig. 1(b), which uses more annotated support images. Although this augmentation in support data generally improves performance, it comes at the expense of requiring more costly manual annotations. Previous studies [2, 3, 4] attribute the superiority of the few-shot segmentation setting to its

*These authors contributed equally to this work.

†Corresponding authors.

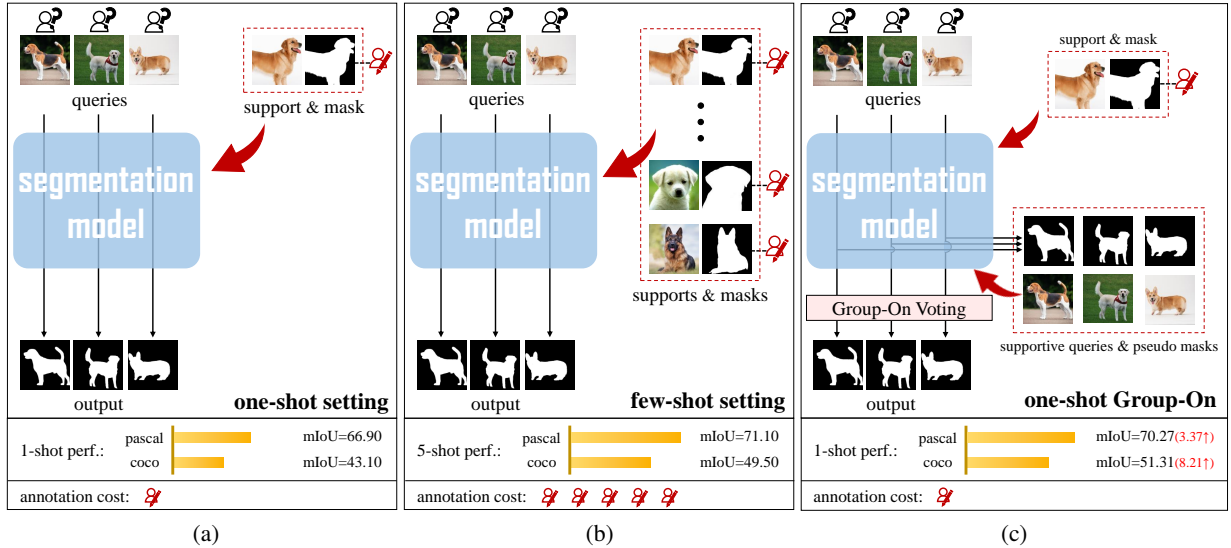


Figure 1: (a) To deal with queries from user, the common 1-shot setting uses one support image annotated by one annotator. (b) The common few-shot setting uses a few support images annotated by many extra annotators. (c) Our one-shot GROUP-ON handles queries in bulk based on ONE labeled support without increasing extra annotators. All the queries are interchangeable and achieve mutual complementary benefits. \blacktriangleleft and \blacktriangleright represent the input of support and pseudo support (*i.e.* supportive queries & pseudo masks), respectively. The bar charts on the bottom show the average segmentation performances on PASCAL-5ⁱ and COCO-20ⁱ datasets. Obviously, our one-shot GROUP-ON even reaches a competitive level with the counterparts under the 5-shot setting.

capability to overcome intra-class object variation, such as the diverse appearances and patterns within one category. The incorporation of additional supports exposes the model to a broader range of category-identical references, thereby introducing greater intra-class diversity, which typically leads to better performance.

Inspired by this, we try to integrate the merits of both one-shot and few-shot settings for fewer annotations and higher performances. Interestingly, a large quantity of query images from the same category can also offer intra-class multiplicity intuitively and thus provide mutual complementary support and benefits, which, however, has been largely neglected in previous research. In this paper, we focus on one-shot segmentation that fixes the number of support images to only ONE. We propose a novel approach for one-shot segmentation, called GROUP-ON, which simultaneously handles multiple queries input by users without increasing extra annotation costs and obtains better performance via mutual assistance among the queries, as seen in Fig. 1(c). For better understanding of this approach, we define the query selected to be predicted as the *host query*, while the rest queries as *supportive queries*. Supportive queries and their intermediate coarse masks, predicted with the only support image, serve as pseudo support data to facilitate segmentation of the host query. In other words, the host query is segmented by the supports from one real support image and multiple pseudo ones (*i.e.*, supportive queries), resulting in multiple coarse prediction candidates. Eventually, such candidate masks for the host query are integrated together to yield the final prediction.

Note that the host and supportive queries hold an equal and interchangeable role. Each one among a group of query images can be the host query to be segmented finally, and all the query images offer favorable information to each other simultaneously. Due to the need for testing many query samples after the deployment of a model in real-world scenarios, it is reasonable and feasible to collect and use various queries and apply GROUP-ON approach for reciprocal help. Since this approach can be viewed as somewhat similar to a “group buying” activity where the individuals benefit from the collective effort, we refer to it as “GROUP-ON”. Experiments show that our approach in the 1-shot setting is even competitive with methods in the 5-shot setting which requires much more time-consuming manual annotations.

In summary, our main contributions are as follows:

- We rethink the real-world application scenarios and propose GROUP-ON, a simple, novel, and effective training approach for one-shot segmentation. GROUP-ON simultaneously processes category-identical queries uploaded by users to leverage the rich object pattern variety to address the intra-class variation issue.
- We propose a Group-On Voting module to assign voting weights to candidate masks based on attention correlations between host and supportive query pairs, which promotes steady training as well. Furthermore, in

the case when not many testing samples are available, we replace attention voting weights with arithmetic mean for lower computational burden.

- We perform extensive experiments and analysis on three challenging FSS benchmarks: PASCAL-5ⁱ [5], COCO-20ⁱ [6], and FSS-1000 [7]. The results show that the performances of one-shot segmentation baselines with our GROUP-ON are comparable to the counterparts of conventional 5-shot segmentation.

2 Related Work

It has been widely acknowledged that OSLSM [8] represents the pioneering work in one-shot segmentation. Inspired by similar architectures for few-shot classification, OSLSM is comprised of a condition branch and a segmentation branch. After that, numerous methods were put forward to improve the performance of FSS, most of which investigated interactions between support and query images while the others focused on details inside either the support or query data.

2.1 Interactions between Support and Queries

Many studies [4, 9, 10] sought to design high-capacity interaction modules between the support and query data. It was common to expand features in multiple scales and layers [11, 12] to enhance in-depth interplay. Based on the Transformer architecture, CyCTR [13], DCAMA [14], and HDMNet [15] developed cross-attention intercommunication while some others [16, 3, 17, 18, 19] did not. Besides, there were some attempts to generate high-dimensional feature correlation tensors, such as HSNet [20], ASNet [1], VAT [21], and DACM [22].

2.2 Support Exploration

Due to the scarcity of reference information, some studies took advantage of the support data in various perspectives (e.g., background and boundaries). PANet [23] proposed to take the predicted query data as pseudo references to segment support images in turn, which aligns both support and query clues and guides each other. As the knowledge of objects from base classes in the background can be ample, it was investigated [24, 25, 26] to use such knowledge to assist novel class predictions. HM [27] and MSI [28] employed two masking techniques to segment more accurate target object boundaries. In addition, IPRNet [29] succeeded in reducing inter-class similarity, but demanded more reference labels even in training under the 5-shot setting, while most methods used five support annotations just in testing. Recently, MIANet [30] introduced supplementary category labels to leverage the general semantic information in a multi-modal manner.

2.3 Query Exploration

For query exploration, DPNet [31] added pseudo-prototypes extracted from the query foreground to the original support prototypes for refinement. SSP [32] suggested that the locality of query masks, which were predicted in high confidence, could aid the support data to segment the leftover low-confidence areas. Unlike the supervised training mode mentioned above, QGNet [33] trained an extractor to approximately locate the targets via global-local contrastive learning.

The known methods on query exploration mainly aimed to make full use of what is inside a single query image to guide the segmentation. In contrast, our GROUP-ON approach exploits directly increasing the query amount to enrich semantic knowledge in an intuitive way. GROUP-ON is more capable and simpler, and can be incorporated seamlessly with plentiful FSS baselines.

3 Methodology

3.1 Problem Setting

Few-shot segmentation (FSS) aims to segment images with limited annotated examples. To improve generalization [34], we adopt the prevalent meta-training paradigm called episodic training [35], following previous work [20, 21]. Concretely, a dataset is divided into two class-disjoint sets \mathcal{D}_{train} and \mathcal{D}_{test} , each of which contains many episodes (an episode usually consists of a query and a support set). What is very particular in FSS is that in an episode, there exist a support set $\mathcal{S} = \{(I^s, M^s)\}$ and a query set $\mathcal{Q} = \{(I^q, M^q)\}$ from the same class, where I^z and M^z represent raw images and their binary masks.

In fact, each episode instantiates an N -way K -shot segmentation task. That is, we select K support image-label pairs per category from N different categories to construct \mathcal{S} . Current approaches typically utilize one support image-label

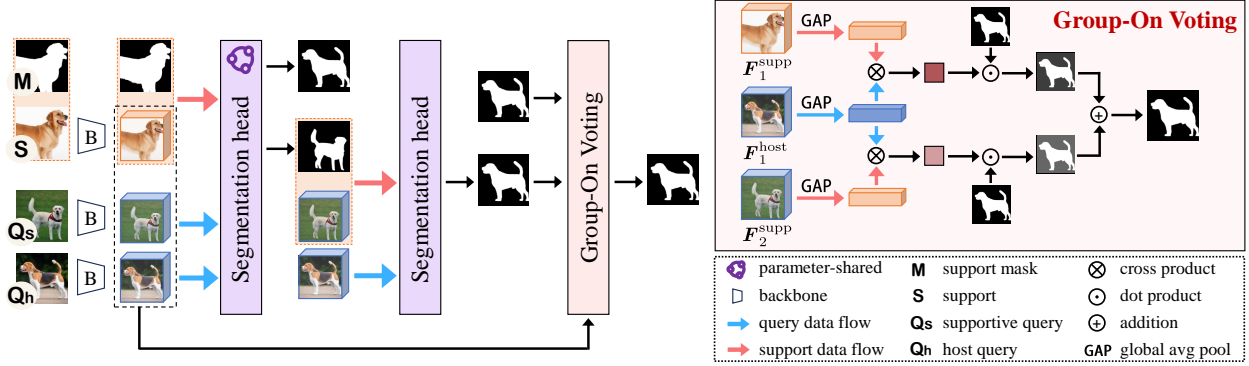


Figure 2: Illustrating GROUP-ON in the one-shot setting. The left is an overview of the proposed approach and we present just one supportive query here for better understanding. Different from the conventional few-shot setting, a group of query images along with one support image is input into the model. After the coarse masks of all the query images are segmented, the supportive image-mask pairs function as pseudo support to segment the host query again. Finally, the Group-On Voting module assigns voting weights to the segmentation masks of the host query and produces the final prediction result. Note that the host and supportive queries play an equal and interchangeable role. For ease of understanding, we present the probability maps in the form of segmentation masks, while they are actually two-dimensional floating-point matrices. The top right corner is details of Group-On Voting module. Note that the input F_1^{supp} , F_2^{supp} , and F^{host} are extracted from a middle layer of the feature extractor.

pair for training whereas one (*i.e.*, 1-way 1-shot) or five (*i.e.*, 1-way 5-shot) for testing, and one query image during both stages. The number of support images matters since it determines the burden of labeling. We always seek to obtain similar performances via as few support images as possible and preferably only one. That is why many models [8, 36] freeze the number of support images to one for training.

In this work, apart from the 1-way setting following [20], we propose and undertake a 1-support C -query setting ($C > 1$) extended from the conventional settings. That is, the amount of support images is ONE but we use multiple query images to support each other in the process.

3.2 Overview of GROUP-ON

The overall pipeline of GROUP-ON is presented in Fig. 2. Basically, it performs one-shot segmentation in three main steps. First, after inputting one support image and query images in a group, we obtain corresponding C predicted masks based on the support data, among which one acts as a candidate mask while the others function as pseudo support masks. Second, given $C - 1$ pseudo support image-mask pairs, the parameter-sharing segmentation head predicts the remaining $C - 1$ candidate segmentation masks. Finally, the Group-On Voting module receives and integrates C candidate masks to produce the final prediction. Below we first describe our approach under the 1-support C -query setting, and then detail the Group-On Voting module.

3.3 Group-On Process under One-Shot Setting

Aiming to maximize the semantic information of different patterns in the same class as much as possible, we use a group of C query images and one support image-label pair as input to the model. The pivotal competitive advantage of GROUP-ON is in utilizing the group of query images for mutual knowledge complement. Among the C query images in the group, the final predicted image is called the host query while the rest images are supportive queries. For simple illustration, in this section we assume that $C = 2$, and the host query and its feature are denoted as I_1^q and F_1^q , while the supportive ones as I_2^q and F_2^q .

The entire data stream goes through the segmentation head Ψ twice. In the first time, the support feature-mask pair (F^s , M^s) and the query features F_i^q 's are input into the model to generate the initial coarse masks, as:

$$\hat{M}^q(i) = \Psi(F^s, M^s, F_i^q), \quad (1)$$

where $\hat{M}^q(i)$ denotes the coarse mask predicted using the real support data (F^s, M^s), $i = 1, 2, \dots, C$ ($C = 2$ here).

Among the initial coarse masks, $\hat{M}^q(1)$ is used as a candidate mask (for the host query), that is:

$$\bar{M}^q(1, 1) = \hat{M}^q(1). \quad (2)$$

$\hat{M}^q(2), \dots, \hat{M}^q(C)$ and their corresponding supportive queries are used as pseudo support data, which are input into the segmentation head again to compute the other candidate masks, as:

$$\bar{M}^q(1, j) = \Psi(F_j^q, \hat{M}^q(j), F_1^q), j = 2, \dots, C, \quad (3)$$

where $\bar{M}^q(1, j)$ is the candidate mask of I_1^q derived from the supportive feature-mask pair $(F_j^q, \hat{M}^q(j))$, $j = 2, \dots, C$. Hence, we obtain C candidate masks $\bar{M}^q(1, 1), \dots, \bar{M}^q(1, C)$, produced from true and pseudo references in distinct appearances but from the same class, thus increasing the object diversity. The final result M_1^q is computed as:

$$M_1^q = \Upsilon(\bar{M}^q(1, 1), \dots, \bar{M}^q(1, C)), \quad (4)$$

where Υ is the Group-On Voting module to be presented in the next subsection.

It is noteworthy that under the 1-shot setting, all the query images are treated equivalently when applying GROUP-ON. That is, the host query is not limited only to I_1^q but must be every query image, and the remaining supportive queries are processed in the same way as what is described above. This process is able to attain mutual knowledge complement. The reason for this is that it allows to make the most out of clues hidden in the query data and promote efficiency.

3.4 Group-On Voting Module

To maximize the utilization of the candidate masks, we develop the Group-On Voting module to vote on each candidate based on the correlations between the host query and the supportive queries/support image for advanced mutual information promotion, which is a process of assigning voting weights. The support image functions similarly as the supportive queries in the Group-On Voting module. Thus, the supportive queries and support image are collectively referred to as supportive query data below for simplicity.

For meta-training, the quality of the coarse masks $\hat{M}^q(i)$, $i = 1, \dots, C$, is woefully poor at the beginning due to non-convergence, which demands stricter filtering on the candidates predicted with the coarse masks. As shown in the top right corner of Fig. 2, we leverage the cross-attention correlations between the host-supportive query pairs to determine how much a candidate mask contributes to the final result during integration. First, from a middle layer of the feature extractor (ResNet50 [37] or ResNet101 [37]), we obtain feature maps $F_1^{\text{host}}, F_i^{\text{supp}} \in \mathbb{R}^{H' \times W' \times C'}$ of the host and supportive queries, for each $i = 1, \dots, C$. Second, we squeeze the feature maps through their spatial dimensions $H' \times W'$ with global average pooling to produce feature vectors $v_1^{\text{host}}, v_i^{\text{supp}} \in \mathbb{R}^{1 \times 1 \times C'}$, $i = 1, \dots, C$. Then following the general form of attention [38], the voting weight w_i is calculated as:

$$w_i = \frac{v_1^{\text{host}} \otimes (v_i^{\text{supp}})^T}{\sqrt{d}}, \quad i = 1, \dots, C, \quad (5)$$

where \otimes is the cross product and d is a hyper-parameter. Here we set $d = 1$. Finally, the voting weights $W = \{w_i\}_{i=1}^C$ activated by the Softmax function are assigned to the C candidate masks $\bar{M}^q(1, i)$'s for the final prediction:

$$M_1^q = \frac{1}{C} \sum_{i=1}^C \bar{M}^q(1, i) * w_i, \quad i = 1, \dots, C, \quad (6)$$

where M_1^q is the final prediction described in Eq. (4).

As for meta-testing, the model is able to segment relatively decent coarse masks after convergence. If we need to reduce the computational requirements of the filtering, we can turn our attention to attaining less computation and faster inference. Thus, the arithmetic mean is employed, as:

$$M_1^q = \frac{1}{C} \sum_{i=1}^C \bar{M}^q(1, i), \quad i = 1, \dots, C, \quad (7)$$

We should emphasize that the host and supportive queries play equal and exchangeable roles, and we take I_1^q as the host query just as an illustrating example here. Different from the few-shot setting, we train and test query images in groups by aiding each other concurrently in the one-shot setting. As the training process progresses, the performance of the model increases gradually and boosts the coarse mask quality, which eventually enhances the final prediction.

Table 1: Segmentation performances on the COCO-20ⁱ (left) and PASCAL-5ⁱ (right) datasets under the 1-support C -query setting. HSNet⁵ and ASNet⁵ represent the results of the baseline models HSNet and ASNet under the conventional 5-support setting, while the rest results are all in the 1-support setting. We highlight the best results in **bold** and underline the second best results for better viewing.

Setting	Method	COCO-20 ⁱ						PASCAL-5 ⁱ					
		Fold-0	Fold-1	Fold-2	Fold-3	Mean	FB-IoU	Fold-0	Fold-1	Fold-2	Fold-3	Mean	FB-IoU
<i>Model performances on the ResNet-50 backbone</i>													
5-support	HSNet ⁵ [20]	43.30	51.30	48.20	45.00	46.90	70.70	70.30	73.20	67.30	67.10	69.50	80.60
	ASNet ⁵ [1]	47.60	50.10	47.70	46.40	47.90	71.60	72.60	74.30	65.30	67.10	70.80	80.40
1-support	SSP [32]	35.50	39.60	37.90	36.70	37.40	-	60.50	67.80	66.40	51.00	61.40	-
	DCAMA [14]	41.90	45.10	44.40	41.70	43.30	69.50	67.50	72.30	59.60	59.00	64.60	75.70
	VAT [21]	39.00	43.80	42.60	39.70	41.30	68.80	67.60	71.20	62.30	60.10	65.30	77.40
	FECANet [4]	38.50	44.60	42.60	40.70	41.60	69.60	69.20	72.30	<u>62.40</u>	<u>65.70</u>	67.40	78.70
	QCLNet [39]	39.80	45.70	42.50	41.20	42.30	-	65.20	70.30	60.80	61.00	64.30	-
	MCE [40]	<u>42.13</u>	48.30	43.68	42.76	44.22	-	65.30	71.22	66.17	61.04	65.93	78.10
	HSNet [20]	36.30	43.10	38.70	38.70	39.20	68.20	64.30	70.70	60.30	60.50	64.00	76.70
	ASNet [1]	41.50	44.10	42.80	40.60	42.40	68.80	68.90	71.70	61.10	62.70	66.10	77.70
	HSNet + GROUP-ON	41.94	<u>48.93</u>	<u>46.66</u>	<u>43.14</u>	<u>45.17 (5.97†)</u>	<u>71.80 (3.60†)</u>	<u>71.32</u>	<u>73.53</u>	61.81	64.18	<u>67.71 (3.71†)</u>	<u>78.75 (2.05†)</u>
	ASNet + GROUP-ON	46.34	49.59	48.60	46.73	47.82 (5.42†)	72.60 (3.80†)	73.07	73.87	61.73	67.71	69.10 (3.00†)	80.05 (2.35†)
<i>Model performances on the ResNet-101 backbone</i>													
5-support	HSNet ⁵ [20]	45.90	53.00	51.80	47.10	49.50	72.40	71.80	74.40	67.00	68.30	70.40	80.60
	ASNet ⁵ [1]	48.00	52.10	49.70	48.20	49.50	72.70	73.10	75.60	65.70	69.90	71.10	81.00
1-support	SSP [32]	39.10	45.10	42.70	41.20	42.00	-	63.20	70.40	68.50	56.30	64.60	-
	DCAMA [14]	41.50	46.20	45.20	41.30	43.50	69.90	65.40	71.40	63.20	58.30	64.60	77.60
	VAT [21]	39.50	44.40	46.10	40.40	42.60	-	68.40	72.50	64.80	64.20	67.50	78.80
	QCLNet [39]	40.00	45.50	45.10	43.60	43.60	-	67.90	72.50	64.30	63.40	67.00	-
	SCCAN [41]	42.60	51.40	<u>50.00</u>	<u>48.80</u>	48.20	69.70	70.00	73.90	<u>66.80</u>	61.70	68.30	78.50
	HSNet [20]	37.20	44.10	42.40	41.30	41.20	69.10	67.30	72.30	62.00	63.10	66.20	77.60
	ASNet [1]	41.80	45.40	43.20	41.90	43.10	69.40	69.00	73.10	62.00	63.60	66.90	78.00
	HSNet + GROUP-ON	<u>44.87</u>	<u>53.44</u>	48.59	47.73	<u>48.66 (7.46†)</u>	<u>73.43 (4.33†)</u>	<u>72.57</u>	<u>74.99</u>	63.53	66.82	<u>69.48 (3.28†)</u>	<u>80.38 (2.78†)</u>
	ASNet + GROUP-ON	48.08	54.18	51.64	51.34	51.31 (8.21†)	73.46 (4.06†)	73.83	75.51	62.48	69.25	70.27 (3.37†)	80.24 (2.24†)

Table 2: Segmentation performance on FSS-1000 [7] in the 1-support C -query setting. HSNet⁵ and ASNet⁵ represent the results of the baseline models HSNet and ASNet in the conventional 5-support setting, while the rest results are all in the 1-support setting. †ASNet: Our reimplementation based on official codes. We mark the best results in **bold**.

Setting	Method	ResNet-50		ResNet-101	
		mIoU	FB-IoU	mIoU	FB-IoU
5-support	HSNet ⁵ [20]	87.50	-	88.50	-
	†ASNet ⁵ [1]	87.28	92.07	88.15	92.65
1-support	SSP [32]	87.30	-	88.60	-
	Anno-free FSS [42]	85.70	-	-	-
	DifFSS [43]	88.40	-	-	-
	HSNet [20]	85.50	-	86.50	-
	†ASNet [1]	85.96	91.04	86.99	91.67
	HSNet + GROUP-ON	87.99	92.62	88.24	92.65
	ASNet + GROUP-ON	88.21	92.63	88.86	93.04

4 Experiments

Datasets. We evaluate our GROUP-ON approach on three standard benchmarks: COCO-20ⁱ [6], PASCAL-5ⁱ [5], and FSS-1000 [7]. Following previous work [20, 44], the experiments on COCO-20ⁱ and PASCAL-5ⁱ are conducted in a cross-validation manner over four folds, with 20 and 5 classes per fold, respectively. For each fold, 1000 episodes are sampled for evaluation, while the rest of the data is used for training. The FSS-1000 dataset containing 1000 classes is divided into 520, 240, and 240 classes for training, validation, and test.

Implementation Details. We incorporate GROUP-ON into two baseline models, HSNet [20] and ASNet [1], denoted as HSNet+GROUP-ON and ASNet+GROUP-ON and they are built upon the PyTorch [46] framework. We use 2 query images for training and 5 for testing, and add the step of alignment regularization [23] to help the training. The backbones ResNet50 [37] and ResNet101 [37], which have been pre-trained on ImageNet [47], are fixed to extract features (features from conv3_x to conv5_x before the ReLU [48] activation of each layer are stacked to form the deep

Table 3: Segmentation Performances on 4 folds of the PASCAL-5ⁱ [5] dataset with CLIP [45] backbone under the 1-support *C*-query setting. †HSNet, †HSNet⁵: Our reimplementations of the baseline model HSNet based on official codes.

Setting	Method	Fold-0	Fold-1	Fold-2	Fold-3	Mean	FB-IoU
5-support	†HSNet ⁵	77.07	82.19	73.43	76.47	77.29	86.49
1-support	†HSNet	72.53	76.38	68.58	69.58	71.77	82.59
	HSNet + GROUP-ON	77.13	80.47	68.82	74.60	75.26 (3.69↑)	84.67 (2.08↑)

Table 4: FPS on 4 folds of the PASCAL-5ⁱ [5] dataset with ResNet50 [37] under the 1-support *C*-query setting. HSNet⁵ represents the results of the baseline model HSNet in the conventional 5-support setting, while the rest results are all in the 1-support setting.

Setting	Method	Fold-0	Fold-1	Fold-2	Fold-3	Mean
5-support	HSNet ⁵ [20]	4.90	4.77	4.77	4.90	4.83
1-support	HSNet [20]	23.33	22.00	21.67	24.00	22.75
	HSNet + GROUP-ON	6.51	6.26	6.34	6.88	6.50

features). In addition, we also experiment with the public pretrained model ViT-L/14@336px of CLIP [45], to evaluate the generalization of our approach on the non-convolutional backbone. In the Group-On Voting module, we select features from the 9th layer as input. The default settings for the optimizer and learning rate of the two baselines remain unchanged. For the batch size, we use 64 for HSNet+GROUP-ON and 48 for ASNet+GROUP-ON. Model training is set to halt when it reaches the maximum 500th epoch. Note that our experiments demonstrate a wide coverage spanning across multiple datasets to various backbones in order to validate the effectiveness and generalizability of our GROUP-ON approach, and they are done on four NVIDIA A100 Tensor Core GPUs for over two months.

Evaluation Metrics. We evaluate the performance with two widely-adopted metrics: mean intersection over union (mIoU) and foreground-background IoU (FB-IoU) [20, 44]. They are computed as:

$$\text{mIoU} = \frac{1}{n} \sum_{i=1}^n \text{IoU}_i, \quad (8)$$

where n is the number of test samples.

$$\text{FB-IoU} = \frac{1}{2}(\text{IoU}_f + \text{IoU}_b), \quad (9)$$

where f means foreground and b means background without regard to the object classes.

4.1 Comparison with State-of-the-Art Methods

4.1.1 Quantitative Results

We compare our results with recent methods [14, 32, 21, 4, 39, 41, 43, 42]. Unless otherwise specified, the reported results of the known methods are all from the original papers. The results in Tab. 1 (left) are on the COCO-20ⁱ dataset and provide the most noticeable gains. Particularly, HSNet+GROUP-ON and ASNet+GROUP-ON with ResNet101 obtain significant improvements of 7.46% and 8.21% on mIoU compared to the counterpart, respectively. The main reason of the superior improvement is the more severe intra-class variation issue derived by the larger data volume in COCO-20ⁱ dataset. Tab. 1 (right) shows the results on the PASCAL-5ⁱ dataset. Our approach delivers consistent improvement (average over 3% in mIoU and 2% in FB-IoU). Tab. 2 represents the results of our approach in the 1-shot setting on the FSS-1000 dataset, which are all competitive with the counterparts in the 5-shot setting. HSNet+GROUP-ON delivers a gain of 2.49% with ResNet50 and 1.74% with ResNet101 in mIoU. Furthermore, Tab. 3 shows the results of our additional experiments with CLIP on the PASCAL-5ⁱ dataset. Given both time and GPU memory considerations, we experiment with one baseline model on one dataset for reference. When using the strong backbone CLIP as the feature extractor, HSNet+GROUP-ON still outperforms the baseline model HSNet by a margin of 3.69% and 2.08% in mIoU and FB-IoU respectively in the 1-shot setting. Such improvements further underscore the capability of our



Figure 3: Some qualitative results on the PASCAL-5ⁱ [5] dataset in the one-shot setting, in the presence of intra-class variation, size differences, duplicated backgrounds, and occlusions.

approach to effectively harness the diversity among queries and demonstrate its broad applicability to any backbone, even the most cutting-edge one.

The inference efficiency of our approach is measured by *frames per second* (FPS). The experiments are carried out on PASCAL-5ⁱ dataset, and we average the results from 5 runs. Regarding the 1-shot setting in Tab. 4, we sacrifice some time cost of inference for better performances. Since our performance enhancement is considerably big and even competitive to the counterparts in the 5-shot setting, its efficiency is acceptable. In comparison to the 5-shot setting, our method is not only more efficient in terms of inference time alone, but also reduces the required manual annotation time for the few-shot setting.

4.1.2 Qualitative Results

To intuitively display our approach, we visualize some results containing challenging intra-class variation under the one-shot setting in Fig. 3. The first row is support images with their masks in blue, while the second row represents the groundtruth. And the following two rows display predictions of the baseline and our approach, respectively. All the images in each column belong to the same category. One can see from our results (the 4th row) that if objects in the support image differ greatly from those in the query images, GROUP-ON captures the semantic essence of the objects and segments more accurately with the reciprocal knowledge help of the multiple query images.

4.2 Ablation Study and Analysis

Extensive ablation experiments from multiple aspects are conducted to provide more insights into our approach, using the PASCAL-5ⁱ [5] dataset and ResNet-50 [37] backbone.

4.2.1 Analysis of Attention Correlations for Group-On Voting

We conduct experiments to validate that cross-attention correlations between the host and supportive query reflect deep relations of image pairs, which guide the assignment of voting weights. We use an indicator ψ to assess the scene differences of two images [26]. Defined by Eq. (10), ψ is the Frobenius norm evaluated on the difference of two Gram matrices [26] \mathbf{G}^h and \mathbf{G}^s :

$$\psi = -\|\mathbf{G}^h - \mathbf{G}^s\|_F, \quad (10)$$

where h and s denote the host query and supportive query, respectively. More complete calculation details are in Appendix A. We randomly sample 100 image pairs from each category and calculate the average results of correlation coefficients for 10 runs. As shown in Fig. 4, the Pearson coefficient [49] and Spearman coefficient [50] between ψ and cross-attention correlations are mostly above 0.5 (which happens for 17 out of 20 for Pearson and 15 out of 20 for Spearman). Such phenomenon indicates a strong connection between the scene difference of images (represented by ψ) and cross-attention correlations (used in Group-On Voting), and thus verifies the effectiveness of the Group-On Voting module.

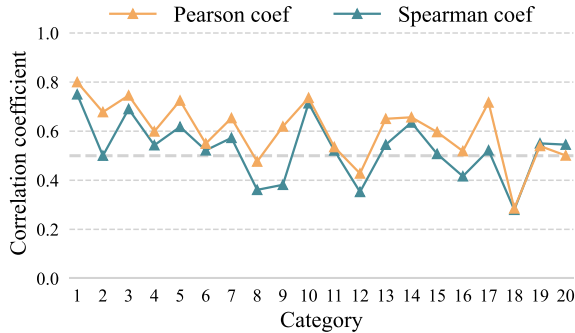


Figure 4: Analysis of attention correlations for Group-On Voting on PASCAL-5ⁱ [5] dataset. We randomly sample many image pairs from totally 20 categories [36] and calculate correlation coefficients between attention correlations and scene differences of image pairs.

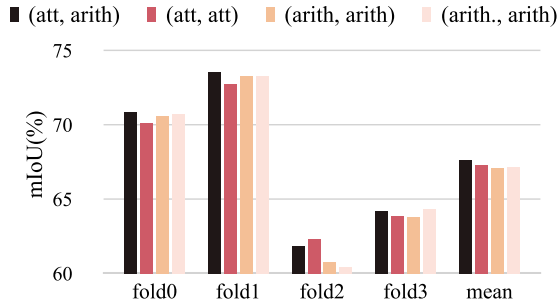


Figure 5: Ablation study on the Group-On Voting weights on the PASCAL-5ⁱ dataset. *att*: cross-attention voting weight scheme. *arith*: arithmetic mean scheme. In the legend, the former one is for training while the latter for testing. We investigate the best combination of *att* and *arith*, and (*att*, *arith*) is the optimal.

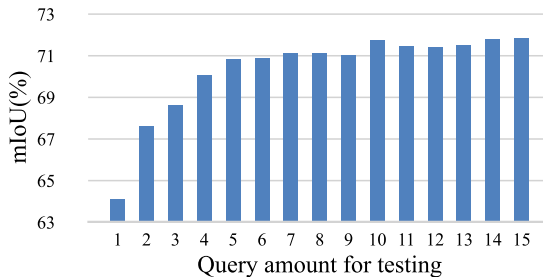
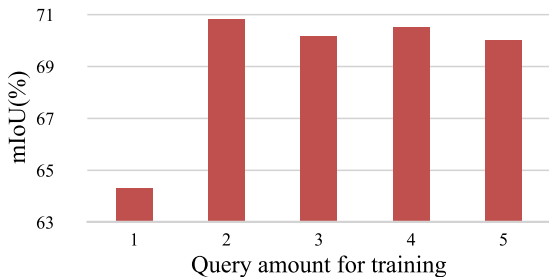


Figure 6: Comparison of the impact of query amounts in training and testing, performed on the fold-0 of PASCAL-5ⁱ. In the left, the best option of query amount for training is 2, given its slight advantage. In the right, with the growth of query amount, the inference performance climbs up and reaches a stable fluctuation. We select 5 queries for testing.

4.2.2 Ablation Study on Voting Weights

We design ablation study to examine how to assign voting weights effectively. The cross-attention voting weight and arithmetic mean schemes are denoted as *att* and *arith* respectively in Fig. 5. In the legend, the former one is for training while the latter for testing. The performance gaps between (*att*, *arith*) and the others on four folds confirm that our proposed option is the best. That is, the Group-On Voting module assigns the voting weights by cross-attention correlations for training, and by arithmetic mean schemes for testing.

4.2.3 Impacts of Query Amounts

We perform comparative experiments using varying numbers of query images during training and testing. Fig. 6 (top) shows that except for the baseline setting (*i.e.*, *amount* = 1), the results of using the other query amounts rise to a similar level and the option of *amount* = 2 wins narrowly. Considering more calculation afflictions as the number of query images increases, we fix the query number to 2 for training here. In Fig. 6 (bottom), with the growth of query number for testing, the performance gradually increases and eventually reaches a stable fluctuation. Due to space limitations, we represent relations between more query amounts and inference performances in Appendix B. For the sake of alignment with the common 5-shot setting and less computation, here we select 5 query images for testing per episode. More exactly, GROUP-ON tests query images in batches of 5 for complementary help of one another. In general, the performance can be improved so long as more query images than one are used, and one may select the most favorable query amount.

5 Conclusions

We proposed a simple and novel approach called GROUP-ON to address the intra-class variation challenge in ONE-shot segmentation. The core innovation of GROUP-ON is to leverage mutual information benefits of query images in a group for more representation multiplicities in a category. Experiments on three standard benchmarks showed

significant performance enhancement and the effectiveness of our approach, which achieved comparable results with the counterparts under the 5-shot setting. In essence, we boosted one-shot segmentation from the data-centric perspective instead of the model architecture design and data labeling. We hold the expectation that our work will shed light on future research in addressing the intra-class variation issue.

References

- [1] Dahyun Kang and Minsu Cho. Integrative few-shot learning for classification and segmentation. In *Conference on Computer Vision and Pattern Recognition*, 2022.
- [2] Xianghui Yang, Bairun Wang, Kaige Chen, Xinchu Zhou, Shuai Yi, Wanli Ouyang, and Luping Zhou. BriNet: Towards bridging the intra-class and inter-class gaps in one-shot segmentation. *arXiv preprint arXiv:2008.06226*, 2020.
- [3] Zhengdong Hu, Yifan Sun, and Yi Yang. Suppressing the heterogeneity: A strong feature extractor for few-shot segmentation. In *International Conference on Learning Representations*, 2023.
- [4] Huafeng Liu, Pai Peng, Tao Chen, Qiong Wang, Yazhou Yao, and Xian-Sheng Hua. FECANet: Boosting few-shot semantic segmentation with feature-enhanced context-aware network. *arXiv preprint arXiv:2301.08160*, 2023.
- [5] Mark Everingham, Luc Van Gool, Christopher Williams, John Winn, and Andrew Zisserman. The pascal visual object classes (VOC) challenge. *International Journal of Computer Vision*, 88:303–338, 2010.
- [6] Tsung-Yi Lin, Michael Maire, Serge Belongie, James Hays, Pietro Perona, Deva Ramanan, Piotr Dollár, and C. Lawrence Zitnick. Microsoft COCO: Common objects in context. In *European Conference on Computer Vision*, 2014.
- [7] X. Li, T. Wei, Y. Chen, Y. Tai, and C. Tang. FSS-1000: A 1000-class dataset for few-shot segmentation. In *Conference on Computer Vision and Pattern Recognition*, 2020.
- [8] Shaban Amirreza, Bansal Shray, Liu Zhen, Essa Irfan, and Boots Byron. One-shot learning for semantic segmentation. In *British Machine Vision Conference*, 2017.
- [9] Joakim Johnander, Johan Edstedt, Michael Felsberg, Fahad Shahbaz Khan, and Martin Danelljan. Dense Gaussian processes for few-shot segmentation. In *European Conference on Computer Vision*, 2022.
- [10] Yuan Wang, Rui Sun, and Tianzhu Zhang. Rethinking the correlation in few-shot segmentation: A buoys view. In *Conference on Computer Vision and Pattern Recognition*, 2023.
- [11] Ehtesham Iqbal, Sirojbek Safarov, and Seongdeok Bang. MSANet: Multi-similarity and attention guidance for boosting few-shot segmentation. *arXiv preprint arXiv:2206.09667*, 2022.
- [12] Alper Kayabaşı, Gökçe Tüfekçi, and İlker Ulusoy. Elimination of non-novel segments at multi-scale for few-shot segmentation. In *Winter Conference on Applications of Computer Vision*, 2023.
- [13] Gengwei Zhang, Guoliang Kang, Yi Yang, and Yunchao Wei. Few-shot segmentation via cycle-consistent Transformer. *arXiv preprint arXiv:2106.02320*, 2022.
- [14] Xinyu Shi, Dong Wei, Yu Zhang, Donghuan Lu, Munan Ning, Jiashun Chen, Kai Ma, and Yefeng Zheng. Dense cross-query-and-support attention weighted mask aggregation for few-shot segmentation. In *European Conference on Computer Vision*, 2022.
- [15] Bohao Peng, Zhuotao Tian, Xiaoyang Wu, Chenyao Wang, Shu Liu, Jingyong Su, and Jiaya Jia. Hierarchical dense correlation distillation for few-shot segmentation. *arXiv preprint arXiv:2303.14652*, 2023.
- [16] Donggyun Kim, Jinwoo Kim, Seongwoong Cho, Chong Luo, and Seunghoon Hong. Universal few-shot learning of dense prediction tasks with visual token matching. In *International Conference on Learning Representations*, 2023.
- [17] Shan Zhang, Tianyi Wu, Sitong Wu, and Guodong Guo. CATrans: Context and affinity Transformer for few-shot segmentation. In *International Joint Conferences on Artificial Intelligence*, 2022.
- [18] Yuanwei Liu, Nian Liu, Xiwen Yao, and Junwei Han. Intermediate prototype mining Transformer for few-shot semantic segmentation. In *Advances in Neural Information Processing Systems*, 2022.
- [19] Yuan Wang, Rui Sun, Zhe Zhang, and Tianzhu Zhang. Adaptive agent transformer for few-shot segmentation. In *European Conference on Computer Vision*, 2022.
- [20] Juhong Min, Dahyun Kang, and Minsu Cho. Hypercorrelation squeeze for few-shot segmentation. In *International Conference on Computer Vision*, 2021.

- [21] Sunghwan Hong, Seokju Cho, Jisu Nam, Stephen Lin, and Seungryong Kim. Cost aggregation with 4D convolutional Swin Transformer for few-shot segmentation. In *European Conference on Computer Vision*, 2022.
- [22] Zhitong Xiong, Haopeng Li, and Xiao Xiang Zhu. Doubly deformable aggregation of covariance matrices for few-shot segmentation. In *European Conference on Computer Vision*, 2022.
- [23] K. Wang, J. Liew, Y. Zou, D. Zhou, and J. Feng. PANet: Few-shot image semantic segmentation with prototype alignment. In *International Conference on Computer Vision*, 2019.
- [24] Boyu Yang, Chang Liu, Bohao Li, Jianbin Jiao, and Qixiang Ye. Prototype mixture models for few-shot semantic segmentation. In *European Conference on Computer Vision*, 2020.
- [25] L. Yang, W. Zhuo, L. Qi, Y. Shi, and Y. Gao. Mining latent classes for few-shot segmentation. In *International Conference on Computer Vision*, 2021.
- [26] Chunbo Lang, Gong Cheng, Binfei Tu, and Junwei Han. Learning what not to segment: A new perspective on few-shot segmentation. In *Conference on Computer Vision and Pattern Recognition*, 2022.
- [27] Seonghyeon Moon, Samuel S. Sohn, Honglu Zhou, Sejong Yoon, Vladimir Pavlovic, Muhammad Haris Khan, and Mubbasir Kapadia. HM: Hybrid masking for few-shot segmentation. In *European Conference on Computer Vision*, 2022.
- [28] Seonghyeon Moon, Samuel S. Sohn, Honglu Zhou, Sejong Yoon, Vladimir Pavlovic, Muhammad Haris Khan, and Mubbasir Kapadia. MSI: Maximize support-set information for few-shot segmentation. *arXiv preprint arXiv:2212.04673*, 2023.
- [29] Atsuro Okazawa. Interclass prototype relation for few-shot segmentation. In *European Conference on Computer Vision*, 2022.
- [30] Yong Yang, Qiong Chen, Yuan Feng, and Tianlin Huang. MIANet: Aggregating unbiased instance and general information for few-shot semantic segmentation. In *Conference on Computer Vision and Pattern Recognition*, 2023.
- [31] Binjie Mao, Xinbang Zhang, Lingfeng Wang, Qian Zhang, Shiming Xiang, and Chunhong Pan. Learning from the target: Dual prototype network for few shot semantic segmentation. In *AAAI Conference on Artificial Intelligence*, 2022.
- [32] Qi Fan, Wenjie Pei, Yu-Wing Tai, and Chi-Keung Tang. Self-support few-shot semantic segmentation. In *European Conference on Computer Vision*, 2022.
- [33] Weide Liu, Zhonghua Wu, Henghui Ding, Fayao Liu, Jie Lin, and Guosheng Lin. Few-shot segmentation with global and local contrastive learning. *arXiv preprint arXiv:2108.05293*, 2021.
- [34] Sachin Ravi and Hugo Larochelle. Optimization as a model for few-shot learning. In *International Conference on Learning Representations*, 2017.
- [35] Oriol Vinyals, Charles Blundell, Timothy Lillicrap, koray kavukcuoglu, and Daan Wierstra. Matching networks for one shot learning. In *Advances in Neural Information Processing Systems*, 2016.
- [36] Xiaolin Zhang, Yunchao Wei, Yi Yang, and Thomas S. Huang. SG-One: Similarity guidance network for one-shot semantic segmentation. *IEEE Transactions on Cybernetics*, 50(9):3855–3865, 2020.
- [37] Kaiming He, Xiangyu Zhang, Shaoqing Ren, and Jian Sun. Deep residual learning for image recognition. In *Conference on Computer Vision and Pattern Recognition*, 2016.
- [38] Ashish Vaswani, Noam Shazeer, Niki Parmar, Jakob Uszkoreit, Llion Jones, Aidan N Gomez, Łukasz Kaiser, and Illia Polosukhin. Attention is all you need. In *Advances in Neural Information Processing Systems*, 2017.
- [39] Zewen Zheng, Guoheng Huang, Xiaochen Yuan, Chi-Man Pun, Hongrui Liu, and Wing-Kuen Ling. Quaternion-Valued correlation learning for few-shot semantic segmentation. *IEEE Transactions on Circuits and Systems for Video Technology*, 33(5):2102–2115, 2023.
- [40] Wenbo Xu, Huaxi Huang, Ming Cheng, Litao Yu, Qiang Wu, and Jian Zhang. Masked cross-image encoding for few-shot segmentation. *arXiv preprint arXiv:2308.11201*, 2023.
- [41] Qianxiong Xu, Wenting Zhao, Guosheng Lin, and Cheng Long. Self-calibrated cross attention network for few-shot segmentation. In *International Conference on Computer Vision*, 2023.
- [42] Sanaz Karimijafarbigloo, Reza Azad, and Dorit Merhof. Self-supervised few-shot learning for semantic segmentation: An annotation-free approach. In *Medical Image Computing and Computer Assisted Intervention*, 2023.
- [43] Weimin Tan, Siyuan Chen, and Bo Yan. DifFSS: Diffusion model for few-shot semantic segmentation. *arXiv preprint arXiv:2307.00773*, 2023.

- [44] Zhuotao Tian, Hengshuang Zhao, Michelle Shu, Zhicheng Yang, Ruiyu Li, and Jiaya Jia. Prior guided feature enrichment network for few-shot segmentation. *IEEE Transactions on Pattern Analysis and Machine Intelligence*, 44(2):1050–1065, 2022.
- [45] Alec Radford, Jong Wook Kim, Chris Hallacy, Aditya Ramesh, Gabriel Goh, Sandhini Agarwal, Girish Sastry, Amanda Askell, Pamela Mishkin, Jack Clark, Gretchen Krueger, and Ilya Sutskever. Learning transferable visual models from natural language supervision. *arXiv preprint arXiv:2103.00020*, 2021.
- [46] Adam Paszke, Sam Gross, Francisco Massa, Adam Lerer, James Bradbury, Gregory Chanan, Trevor Killeen, Zeming Lin, Natalia Gimelshein, Luca Antiga, Alban Desmaison, Andreas KÄpf, Edward Yang, Zach DeVito, Martin Raison, Alykhan Tejani, Sasank Chilamkurthy, Benoit Steiner, Lu Fang, Junjie Bai, and Soumith Chintala. PyTorch: An imperative style, high-performance deep learning library. In *Advances in Neural Information Processing Systems*, 2019.
- [47] Jia Deng, Wei Dong, Richard Socher, Li-Jia Li, Kai Li, and Li Fei-Fei. ImageNet: A large-scale hierarchical image database. In *Conference on Computer Vision and Pattern Recognition*, 2009.
- [48] Xavier Glorot, Antoine Bordes, and Yoshua Bengio. Deep sparse rectifier neural networks. In *International Conference on Artificial Intelligence and Statistics*, 2011.
- [49] Karl Pearson. Notes on regression and inheritance in the case of two parents. In *Royal Society of London*, 1895.
- [50] C. Spearman. The proof and measurement of association between two things. *The American Journal of Psychology*, 15(1):72–101, 1904.

A Analysis of Attention Correlations for Group-On Voting

First, the low-level feature maps $\mathbf{F}_{\text{low}}^h, \mathbf{F}_{\text{low}}^s \in \mathbb{R}^{H_1 \times W_1 \times C_1}$ of the host query and supportive query are extracted from the 3th layer of the total features. Then we reshape them and calculate the Gram Matrices, following the previous work[26]. Please note that the relevant operations of these two queries are similar, and that of the host one can be summarized as:

$$\mathbf{A}_h = \mathcal{F}_{\text{reshape}}(\mathbf{F}_{\text{low}}^h) \in \mathbb{R}^{C_1 \times N_1}, \quad (11)$$

$$\mathbf{G}^h = \mathbf{A}_h \mathbf{A}_h^T \in \mathbb{R}^{C_1 \times C_1}, \quad (12)$$

where $N_1 = H_1 \times W_1$ and $\mathcal{F}_{\text{reshape}}$ reshapes the size of input tensor to $C_1 \times N_1$.

B Comparison of Using Different Query Amounts for Testing

To further investigate the impact of varying query amounts during testing, we carry out supplementary experiments using larger numbers of query images. In Fig. 7, as the number of query images varies from 1 to 30, the inference performance climbs up and remains relatively stable without any noticeable downtrends. However, the inference time per query manifests a sustainable growth. Such trends indicate a marginal performance improvement at the cost of significant computational resources after reaching a point of stable fluctuation. In light of the inference efficiency, it is not a viable strategy to increase the query amount without restrictions. Instead, one should select the most favorable query amount that balances both efficiency and performance. In this paper, we set the query amount to 5 during testing.

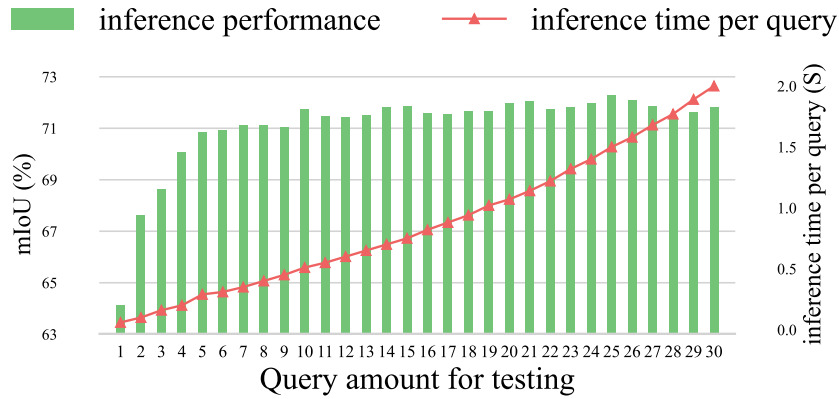


Figure 7: Supplementary study on the impact of query amounts for testing performed on fold-0 of the PASCAL-5ⁱ [5] dataset.